

- were rated as significant if the χ^2 reduction of the fitting procedure exceeded 15% and a z score of >3 was reached, corresponding to a probability of <0.0027 of detection of false positive peaks.
18. LFPs were recorded from the same microelectrodes as MUA by differential filtering (1 to 100 Hz, 3 dB per octave) and digitized at a sampling rate of 1 kHz. Power spectra were computed with a resolution of 0.5 Hz and normalized to the total power between 0.1 and 100 Hz. Frequencies between 47.5 and 52.5 Hz were routinely excluded from analysis, and in the figures they are displayed as linear interpolation between flanking values. The sample of sufficiently noise-free data was recruited from $N = 35$ recording site pairs (see Fig. 2F). To assess the desynchronizing effect of MRF stimulation, we computed the power spectra of the LFPs before and after MRF stimulation from the same periods of light responses used for cross-correlation analysis and from periods of spontaneous activity that had the same duration.
 19. In the entire sample, MRF stimulation enhanced the relative (normalized) power of the LFPs in frequency bands above 14 Hz during periods of both spontaneous and light-evoked activity [beta (14 to 30 Hz) and gamma (>30 Hz), $P < 0.05$ in a one-sample t test] and decreased the power in the low-frequency bands for spontaneous activity [alpha (8 to 13 Hz), $P < 0.001$], theta (4 to 7 Hz, $P < 0.01$), and delta (1 to 3 Hz, $P < 0.05$]). For periods of light-evoked activity, the relative decrease of power in the low-frequency range (<14 Hz) reached significance [alpha ($P <$

- 0.05), theta ($P < 0.01$), and delta ($P < 0.01$)] only for responses to coherent visual stimuli that also induced response synchronization, but not when compared across all stimulation conditions.
20. For our sample of 760 recording sequences, in which visual coactivation yielded at least 1.5 times as many spikes during responses as during spontaneous activity in five subsequent stimulus presentations, averaged PSTHs and cross-correlograms were computed for the responses to these five stimulus presentations (example in Fig. 2, A to D). Of these 760 sequences, 134 sequences originating from 48 pairs of recording sites showed significant correlation in at least one of the four blocks; 85 sequences were recorded with coherent and 49 with noncoherent visual stimulation (see Fig. 3). A robust measure for correlation strength, which is close to the mean percentage increase in firing probability [see T. C. Cope, E. E. Fetz, M. Matsumura, *J. Physiol. (London)* **390**, 161 (1987)], is the relative modulation amplitude (RMA) of the center peak in the correlogram, defined as the ratio of its height to the mean of the correlation function, expressed either as a real number between 0 and 1 or as a percentage. Computing the differences of RMA preserves the identity of individual measurement series before pooling. For the same reason, power changes in the gamma frequency band of the LFP are also expressed as differences. Because we had multiple measurement sequences (2.8 on average) for most of the recording site pairs, data are presented (Figs.

- 2, E and F, and 3E) and used in statistical evaluation as average values per pair. We did not normalize the correlograms for the number of stimulus presentations because this would provide no additional information and because the number of trials for each recording sequence (4 times 5) was the same.
21. The analysis was restricted to those cases where spontaneous fluctuations in correlation strength (RMA) remained within 1 SD of the entire distribution, which corresponded to a value of 0.251 RMA. This requirement was met by 64 of 85 recording sequences during coherent visual stimulation and by 38 of 49 recording sequences during noncoherent visual stimulation. Data for correlation changes during noncoherent visual stimulation without MRF activation are not shown.
22. C. Schwarz and J. Bolz, *J. Neurosci.* **11**, 2995 (1991); J. I. Nelson, P. A. Salin, M. H. J. Munk, M. Arzi, J. Bullier, *Visual Neurosci.* **9**, 21 (1992); P. König, A. K. Engel, S. Löwel, W. Singer, *Eur. J. Neurosci.* **5**, 501 (1993); M. H. J. Munk, L. G. Nowak, J. I. Nelson, J. Bullier, *J. Neurophysiol.* **74**, 2401 (1995).
23. P. König, A. K. Engel, W. Singer, *Proc. Natl. Acad. Sci. U.S.A.* **92**, 290 (1995); A. K. Engel, P. König, T. B. Schillen, *Curr. Biol.* **2**, 332 (1992).
24. W. Singer, *Science* **270**, 758 (1995).
25. We thank S. Herzog and H. Klon-Lipok for help with the experiments, M. Sum and E. Raulf for expert histology, and R. Ruhl for support with the graphics.

4 October 1995; accepted 6 February 1996

Short-Term Plasticity of a Thalamocortical Pathway Dynamically Modulated by Behavioral State

Manuel A. Castro-Alamancos* and Barry W. Connors

The neocortex receives information about the environment and the rest of the brain through pathways from the thalamus. These pathways have frequency-dependent properties that can strongly influence their effect on the neocortex. In 1943 Morison and Dempsey described "augmenting responses," a form of short-term plasticity in some thalamocortical pathways that is triggered by 8- to 15-hertz activation. Results from anesthetized rats showed that the augmenting response is initiated by pyramidal cells in layer V. The augmenting response was also observed in awake, unrestrained animals and was found to be dynamically modulated by their behavioral state.

Synaptic pathways originating in the thalamus provide sensory and motor information to the neocortex (1, 2). The response characteristics of these pathways are not static but display short-term plasticity (that is, frequency-dependent properties). Thalamocortical pathways are known to be modulated during sleep-wake cycles (1, 2), but the regulation of their plasticity during different waking states has not been studied previously. If this short-term plasticity varied dynamically with behavioral state, the capacity for information processing could be increased. In 1943 Morison and Dempsey showed that low-frequency (8- to 15-Hz) activation of certain thalamic pathways

causes a progressively "augmenting response" in the neocortex (3). This robust form of short-term plasticity has been demonstrated repeatedly in both motor (4) and sensory (5) regions of the neocortex. But despite extensive study, there is no consensus regarding the mechanisms of the augmenting response (6) or its relation to behavior. We have investigated the augmenting response in a synaptic pathway from the ventrolateral nucleus (VL) of the thalamus to the sensorimotor neocortex and explored its mechanisms and modulation by behavioral state.

Single electrical stimuli delivered to the VL of the anesthetized rat evoked a characteristic field potential in the depth of the parietofrontal cortex (Fig. 1A) (7). A short-latency primary response was followed 175 to 200 ms later by a long-latency potential. Paired stimuli, separated by 100 ms, gener-

ated an augmenting response (Fig. 1B); the second response at this interval was several times larger than the first and was also followed by the long-latency potential. The narrow effective time window for generating an augmenting response, illustrated in Fig. 1C, was between about 50 ms and the peak of the long-latency potential (200 ms), after which the second response was not augmented. Current-source density (CSD) analysis revealed that the primary VL response, the onset of the augmenting response, and the long-latency potential were all generated by neurons of layer V (Fig. 1D). After the onset of the augmenting response, strong current sinks spread quickly into upper cortical layers and horizontally into adjacent cortical regions. The area of horizontal spread of the augmenting response in the frontoparietal neocortex is shown in Fig. 1E (8).

The relevance of the augmenting response to behavior has not been demonstrated, although the response has been shown to vary between sleep and waking (9). We found that the VL-generated augmenting response was strong and reliable in awake, unrestrained rats, with characteristics virtually identical to those observed in anesthetized animals (Fig. 2A, "resting"). However, the augmenting response, but not the primary response, was strongly influenced by the behavioral state of the animal. Three states were distinguished in awake rats that were allowed to move freely about an open field (10): resting, exploration, and immobility. The augmenting response was strong when the animal was resting (but not sleeping), but strongly suppressed when the animal was moving about and actively exploring the environment (Fig. 2A, "explo-

Department of Neuroscience, Brown University, Providence, RI 02912, USA.

* To whom correspondence should be addressed.
E-mail: manuel_castro@brown.edu

ration"). In addition, during brief periods of immobility that occurred phasically during exploration periods, a strong augmenting response reappeared (Fig. 2A, "immobility"). The variability of both primary and VL-evoked augmenting responses, and their correspondence with the animal's motor activity, during a 45-min recording session with one rat are shown in Fig. 2, B and C. Similar observations were made in 15 rats. Data from another rat (Fig. 2D) show the loss of the augmenting response during a session of skilled motor behavior, during which a previously trained animal was allowed to reach out of the cage with his forelimb into a tube to grasp food pellets (11).

Initial studies of the augmenting response suggested that it was generated by mechanisms within the thalamus, but more recent work has attributed it to neocortical processes (5, 12). We found that blocking neural activity in the thalamus did not influence the augmenting response (12). We explored the cellular mechanisms of the augmenting response with intracellular and extracellular recordings in the neocortex of anesthetized rats (13). The effect of stimulating the VL with one pulse while recording from the soma of a layer V neuron is shown in Fig. 3A. The

short-latency (primary) response was a small excitatory postsynaptic potential (EPSP), which was terminated sharply by a strong, hyperpolarizing inhibitory PSP (IPSP). The IPSP was interrupted by a long-latency depolarizing potential that peaked at 200 ms. A second VL stimulus delivered during the IPSP and before the peak of the long-latency potential (that is, between 50 and 200 ms) triggered an augmented EPSP, which was strong enough to evoke action potentials (Fig. 3B); stimuli delivered during or after the long-latency depolarization were not augmented. All cells recorded in the sensorimotor cortex in response to VL stimulation displayed an augmenting response, although with different latencies (see below). The profile of extracellular currents revealed by CSD analysis (Fig. 1D) indicated a central role for layer V cells in the initiation of the augmenting response. Comparisons of sequentially recorded (that is, in the same electrode penetration) layer V, layer III, and extracellular potentials *in vivo* reinforced this conclusion (Fig. 3C). Thus, somatic responses from layer V cells were phase-locked to the shortest latency component of the concurrently recorded field potential from layer V (Fig. 3C). Responses of cells from other layers displayed longer latencies, indicating that they could not be triggering

the augmenting response. Layer III cell responses were phase-locked with the peak extracellular negativities recorded within that layer (Fig. 3C).

These results indicate that the augmenting response is generated in layer V and that the hyperpolarization of layer V cells plays an important role in the underlying cellular mechanisms. Axons from the VL terminate within layer V (14) and directly excite both pyramidal cells and inhibitory interneurons in layer V. The ensuing strong hyperpolar-

Fig. 1. Stimulation of the VL-to-cortex synaptic pathway induces an augmenting response. (A) Field potential response recorded at a depth of 1000 μm in the sensorimotor neocortex in response to stimulation of the VL of the thalamus with a single current pulse. (B) An augmenting response is induced in response to a second pulse delivered at a 100-ms interval. (C) Augmenting responses are only induced at an interval between 50 ms and the peak of the long-latency potential (175 to 200 ms). The second pulse was delivered at different intervals (15, 25, 50, 100, 150, 200, 250, and 300 ms) with respect to the first pulse (red trace). (D) Current-source density (CSD) analysis of the primary response, augmenting response, and long-latency potential. The sink (reds and yellows) and source (blues) distribution indicates that layer V pyramidal cells are activated by VL stimulation and are responsible for the generation of the augmenting response and long-latency potential. (E) Contour plot of the peak amplitude of the negative field potential recorded in the depth (1500 μm) of the neocortex at 24 equally spaced (1 mm) electrode penetrations in the frontoparietal neocortex in response to the first and second (augmenting response) pulses delivered at a 100-ms interval. Coordinates are given with respect to bregma and the midline.

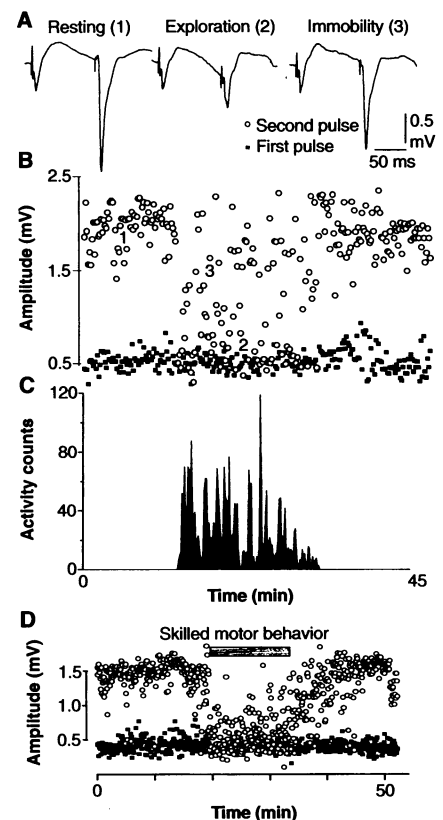
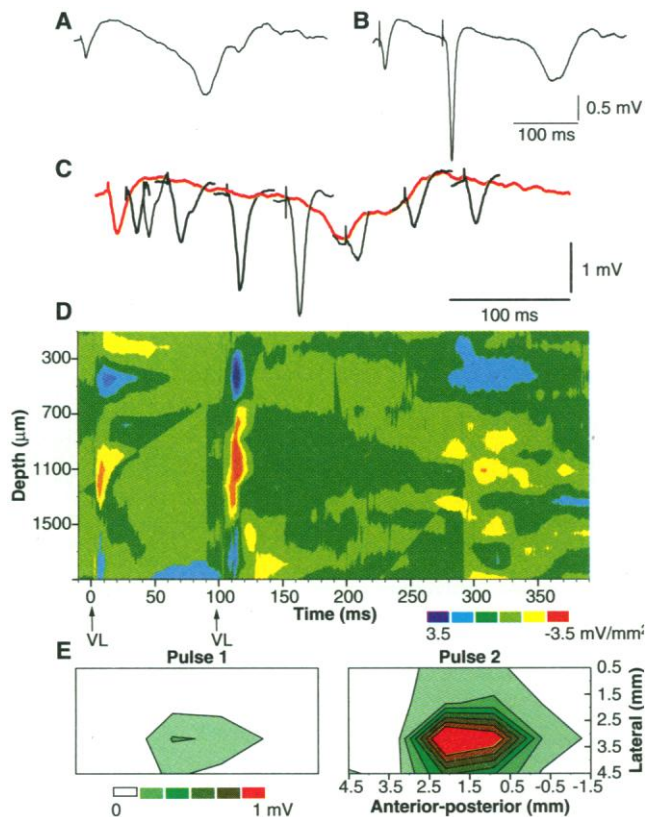
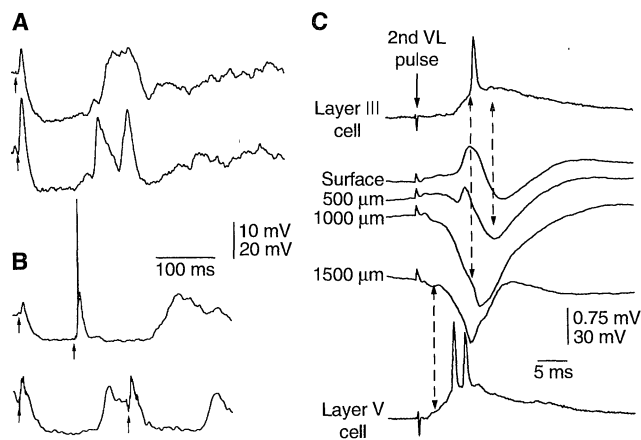


Fig. 2. Dynamic modulation of the augmenting response with behavioral state in awake, freely moving animals. (A) An augmenting response is induced during periods of resting and immobility but is inactivated during periods of exploration. The numbers in parentheses indicate the location of the trace in (B). (B) An animal was allowed to freely explore an open field while motor activity was monitored with photobeam detectors. Paired pulses at a 100-ms interval were applied to the VL (100 μA) at 0.1 Hz, and responses were recorded in the sensorimotor neocortex. (C) The amplitudes of the first (closed squares) and second (open circles) responses were measured and plotted with respect to the level of motor activity displayed by the animal as indicated by the number of photobeam interruptions (activity counts) per 10-s bins. (D) An animal was trained to grasp food pellets with his forelimb by reaching into a tube outside of the cage. During the period that the animal performed this skilled motor behavior the augmenting response was largely inactivated. Paired pulses at a 100-ms interval were delivered to the VL (60 μA) at 0.2 Hz.

Fig. 3. Intracellular correlates of the augmenting response in vivo. **(A)** Intracellular recordings of a layer V cell in the sensorimotor neocortex in response to VL stimuli (arrows) produce a small EPSP that is truncated by a strong hyperpolarization and followed by a rebound depolarizing potential. The upper trace was recorded at resting membrane potential, whereas the lower trace was recorded with negative current injection that hyperpolarized the cell by 20 mV. **(B)** A second pulse delivered during the IPSP phase, and before the peak of the rebound potential, generated an augmented response. Shown are two traces from a layer V cell corresponding to 100- and 200-ms intervals. **(C)** The augmented response corresponding to the second pulse of a pair delivered to the VL is shown. Sequential recordings (same penetration) from cells in different layers are phase-locked to different components of the field potentials recorded extracellularly. Responses of layer V cells correspond to the earlier component of the augmenting response recorded extracellularly between 1000 and 1500 μm , whereas recordings from layer III cells correspond to later components of the field potentials recorded in the upper layers.



ization of layer V pyramidal cells, generated by this feedforward inhibition (15), may activate or deactivate voltage-dependent conductances in layer V cells (16) that could initiate the augmenting response and spread it through local synaptic networks.

These results also show that the augmenting response is dynamically modulated during transitions between awake behavioral states. During active exploration or skilled behavioral performance, the augmenting response was inactivated. This type of modulation is selective, because the primary responses to VL stimulation were not affected. The mechanisms of this modulation are unknown, but they may involve diffuse transmitter systems (for example, acetylcholine and norepinephrine) that are activated during exploration and arousal (17). Stimulation of the midbrain reticular formation can rapidly modulate augmenting responses in anesthetized animals (18). The augmenting response may be involved in generating the 7- to 12-Hz cortical oscillations associated with awake immobility (19); these spontaneous rhythms and the augmenting response both coincidentally terminate with the onset of movement. Loss of the augmenting response during active exploration should profoundly affect the pattern of activity flowing between thalamus and neocortex. Dynamic modulation of short-term thalamocortical plasticity may allow rapid switching between different information processing modes depending on behavioral contingencies.

REFERENCES AND NOTES

1. E. G. Jones and A. Peters, Eds., *Cerebral Cortex* (Plenum, New York, 1986), vol. 5.
2. M. Steriade, E. G. Jones, R. R. Llinas, *Thalamic Os-*

illations and Signaling (Wiley, New York, 1990).

3. E. W. Dempsey and R. S. Morison, *Am. J. Physiol.* **138**, 283 (1943); R. S. Morison and E. W. Dempsey, *ibid.*, p. 297. Augmenting responses are neocortical field potentials, characteristically surface positive and middle-layer negative, that increase in size during paired or multiple stimuli applied at 8 to 15 Hz; steady state is reached by the third response. Augmenting responses should not be confused with recruiting responses, which are surface negative and middle-layer positive and are induced by stimulating thalamic nuclei that project to neocortical layer I [L. L. Glenn, J. Hada, J. P. Roy, M. Deschenes, M. Steriade, *Neuroscience* **7**, 1861 (1982); M. Herkenham, in (1), pp. 403-446], nor with a different form of short-term synaptic plasticity commonly known as augmentation [R. S. Zucker, *Annu. Rev. Neurosci.* **12**, 13 (1989)].
4. W. A. Spencer and J. M. Brookhart, *J. Neurophysiol.* **24**, 26 (1961); D. P. Purpura and R. J. Shofer, *ibid.* **27**, 117 (1964); K. Sasaki, H. P. Staunton, G. Dieckmann, *Exp. Neurol.* **26**, 369 (1970).
5. D. Morin and M. Steriade, *Brain Res.* **205**, 49 (1981); D. Ferster and S. Lindstrom, *J. Physiol.* **367**, 217 (1985).
6. Explanations have included origins in the thalamus (3) and the cortex (5).
7. Sprague-Dawley rats (250 to 350 g) were anesthetized with ketamine HCl (100 mg per kilogram of body weight, intraperitoneally) and regularly supplemented (50 mg/kg, intramuscularly). After induction of surgical anesthesia, the animal was placed in a stereotaxic frame. All skin incisions and frame contacts with the skin were injected with lidocaine (2%). A unilateral craniotomy extended over a large area of the parietofrontal cortex. Small incisions were made in the dura as necessary, and the cortical surface was covered with saline. Body temperature was monitored and maintained constant with a heating pad. Thalamus-stimulating electrodes were inserted with stereotaxic procedures [all coordinates are given in millimeters, in reference to the bregma and the dura] [G. Paxinos and C. Watson, *The Rat Brain in Stereotaxic Coordinates* (Academic Press, New York, 1982)]. Coordinates for the VL were approximately (in millimeters) anterior-posterior = -2.0; lateral = 2.0; and depth = 5.5. Stimulus current intensity was selected to induce a stable response (<200 μA), and pulses were monophasic and of 200- μs duration. Twisted, insulated bipolar stainless steel electrodes were used for stimulating the thalamus. Recording electrodes were placed within the following region: anterior-posterior = 0 to 1 mm, and lateral = 3 to 4 mm. Extracellular

recording electrodes were Teflon-insulated platinum-iridium wires (0.007-inch diameter, 0.005-inch tip size). For CSD analysis, 20 responses were averaged from each depth, with averages taken at 100- μm intervals from the pial surface to a depth of 2000. CSDs were calculated by approximating the second spatial derivative of voltage with methods previously described [J. Mitzdorf, *Physiol. Rev.* **65**, 37 (1985)]. To ensure stability of the preparation during long recording sessions, we did the following: (i) the moving electrode was always returned to the initial recording depths, (ii) measurements from that site were repeated to check that no significant change had occurred, and (iii) the electrocorticogram was continuously monitored for stability. Electrophysiological responses were sampled at 10 kHz and stored on a computer with Experimenter's Workbench (Data Wave Technologies). Analysis was performed with Experimenter's Workbench and Origin (Microcal Software). At the end of each experiment, marking lesions were placed at the thalamic locations that had served as stimulating sites. The animals were given an overdose of sodium pentobarbital, and the brain was extracted and placed in a fixative solution (5% paraformaldehyde in saline). Subsequently, slices of the frontoparietal cortex and thalamus were cut with a vibratome and stained for Nissl. Protocols for all experiments were approved by the Brown University Institutional Animal Care and Use Committee.

8. Recordings were made from a grid of 24 equally spaced (1 mm apart) penetrations across the frontoparietal neocortex of the rat. Figure 1E shows the amplitude of the negative field potential recorded in the depth (1500 μm) of the cortex in response to the first and second pulse delivered to the VL with an interstimulus interval of 100 ms.
9. M. Steriade, G. Iosif, V. Apostol, *J. Neurophysiol.* **32**, 251 (1969).
10. Procedures for implanting electrodes in freely moving animals have been described [M. A. Castro-Alamancos and J. Borrell, *Neuroscience* **68**, 793 (1995)]. Electrophysiological recordings were performed as in anesthetized animals, but with field effect transistors (NLABS, Dennison, TX) attached to the recording electrodes within the animal's head connector. During recording sessions an animal was placed in an open field (43.2 cm by 43.2 cm) containing two arrays of 16 photobeams (Med Associates, Georgia, VT) that detected any movements performed by the animal in the open field. Electrophysiological recordings, motor activity consisting of 10-ms pulses signaling the interruption of a photobeam, and the experimenter's observations were fed into a video tape recording system (Neurodata Instruments, New York, NY) and to Experimenter's Workbench. Three awake behavioral states were easily distinguished. During the immobility state the animal was standing still with eyes open and fixed (photobeams were not interrupted). Immobility preceded the onset of the exploration state, during which the animal moved around and explored the environment (large numbers of photobeam interruptions are recorded). Finally, during the resting state the animal was lying down in the cage, typically in one corner, with eyes open (no photobeam counts were detected). The resting state was easily distinguished from immobility by visual observation and by the long period of associated photobeam silence, whereas during immobility, phasic periods of photobeam silence were interrupted by periods of exploration.
11. Animals had been trained in a motor skill grasping task [M. A. Castro-Alamancos and J. Borrell, *Neuroscience* **52**, 637 (1993)] for several days before being implanted with stimulating and recording electrodes. During the recording sessions the animals were allowed to grasp food pellets for a continuous session of 10 to 15 min. While food was accessible, the animals were very actively engaged in reaching into the tube, grasping and retrieving food pellets, and placing the pellets into their mouths, and immobility did not occur.
12. M. A. Castro-Alamancos and B. W. Connors, *J. Neurosci.* **16**, 2767 (1996).
13. Intracellular (conventional sharp-type) recording electrodes were filled with 3 M potassium acetate (80

to 120 megaohms), recordings were made from cells of different cortical layers ($n = 41$), and procedures were similar to those used for slices [M. A. Castro-Alamancos, J. P. Donoghue, B. W. Connors, *J. Neurosci.* **15**, 5324 (1995)].

14. M. Herkenham, *Science* **207**, 532 (1980).

15. B. W. Connors, R. C. Malenka, L. R. Silva, J. Physiol. **406**, 443 (1988); P. Somogyi, in *Neural Mechanisms of Visual Perception*, D. M. Lam and C. D. Gilbert, Eds. (Gulf, Houston, TX, 1990), pp. 35–62.; A. Ag-

mon and B. W. Connors, *J. Neurosci.* **12**, 319 (1992).

16. L. R. Silva, Y. Amitai, B. W. Connors, *Science* **251**, 432 (1991); Z. Wang and D. A. McCormick, *J. Neurosci.* **13**, 2199 (1993).

17. G. Aston-Jones and F. E. Bloom, *J. Neurosci.* **1**, 876 (1981); J. R. Cooper, F. E. Bloom, R. H. Roth, *The Biochemical Basis of Neuropharmacology* (Oxford Univ. Press, New York, 1991).

18. M. Steriade and D. Morin, *Brain Res.* **205**, 67 (1981).

19. K. Semba and B. R. Komisaruk, *Neuroscience* **12**,

761 (1984); C. H. Vanderwolf, *Int. Rev. Neurobiol.* **30**, 225; M. A. L. Nicoletis, L. A. Baccala, R. C. S. Lin, J. K. Chapin, *Science* **268**, 1353 (1995).

20. Supported by fellowships to M.A.C. from the Ministry of Science and Education of Spain and the National Institute of Mental Health (MH19118), and grants to B.W.C. from the NIH (NS25983) and the Office of Naval Research (N00014-90-J-1701).

29 September 1995; accepted 8 February 1996

Rho1p, a Yeast Protein at the Interface Between Cell Polarization and Morphogenesis

Jana Drgonová, Tomás Drgon, Kazuma Tanaka, Roman Kollár, Guang-Chao Chen, Richard A. Ford, Clarence S. M. Chan, Yoshimi Takai, Enrico Cabib*

The enzyme that catalyzes the synthesis of the major structural component of the yeast cell wall, $\beta(1\rightarrow3)$ -D-glucan synthase (also known as 1,3- β -glucan synthase), requires a guanosine triphosphate (GTP) binding protein for activity. The GTP binding protein was identified as Rho1p. The *rho1* mutants were defective in GTP stimulation of glucan synthase, and the defect was corrected by addition of purified or recombinant Rho1p. A protein missing in purified preparations from a *rho1* strain was identified as Rho1p. Rho1p also regulates protein kinase C, which controls a mitogen-activated protein kinase cascade. Experiments with a dominant positive *PKC1* gene showed that the two effects of Rho1p are independent of each other. The colocalization of Rho1p with actin patches at the site of bud emergence and the role of Rho1p in cell wall synthesis emphasize the importance of Rho1p in polarized growth and morphogenesis.

Little is known at the molecular level about the mechanisms involved in morphogenesis, a fundamental process in growth and differentiation. To study those mechanisms, we have used the cell wall of the yeast *Saccharomyces cerevisiae* (1). In the yeast budding cycle, synthesis of a new cell wall starts at bud emergence and continues until the daughter cell completes its maturation, after cytokinesis and septum formation (1). Temporal controls must be in place to ensure synchronization between cell wall growth and the cell cycle. Spatial regulation is also required to determine the site where the new bud will emerge (2) and to direct growth of the cell wall in an orderly manner that will result in the correct shape for the new cell. To gain information about such controls, we have studied the biosynthesis of $\beta(1\rightarrow3)$ glucan, the major structural component of the yeast cell wall (1). $\beta(1\rightarrow3)$ Glucan synthase (GS), a membrane-bound enzyme, is stimulated by submicromolar concentrations of GTP (3).

J. Drgonová, T. Drgon, R. Kollár, R. A. Ford, E. Cabib, Laboratory of Biochemistry and Metabolism, National Institute of Diabetes and Digestive and Kidney Diseases, Building 10, Room 9N-115, Bethesda, MD 20892, USA. K. Tanaka and Y. Takai, Department of Molecular Biology and Biochemistry, Osaka University Medical School, 2-2 Yamada-oka, Suita, Osaka 565, Japan. G.-C. Chen and C. S. M. Chan, Department of Microbiology, University of Texas, Austin, TX 78712, USA.

*To whom correspondence should be addressed.

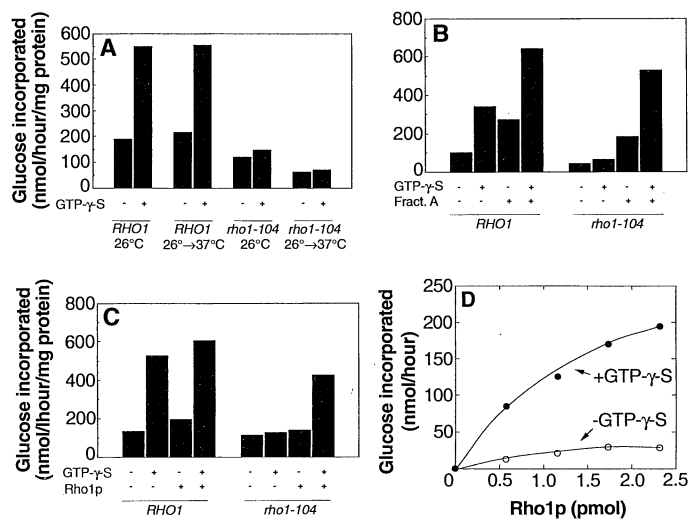
A proteinaceous component that interacts with GTP has been extracted from membranes of several fungi (4).

Recently, two fractions, A and B, both essential for GS activity, were solubilized from yeast membranes and a GTP binding protein was purified from fraction A (5). To identify this protein, we tested mutants in

known small GTP binding proteins. Of the approximately 20 such proteins found thus far in yeast, most participate in intracellular traffic. However, defects in the *RHO1* (6) and *RHO3* or *RHO4* (7) genes result in arrest of the cell cycle at the small bud stage with concomitant cell lysis (8, 9), a phenotype consistent with a defect in the initiation of cell wall growth caused by impaired glucan synthesis.

Here, we measured GS activity in the absence or presence of guanosine-5'-O-(3-thiotriphosphate) (GTP- γ -S) in membrane preparations from strains containing a temperature-sensitive mutation in *RHO1*, *rho1-104* (8). Strains with a conditional mutation in *RHO3* and a disruption in *RHO4* (or vice versa) were also tested. Enzymatic activity and GTP stimulation of the synthase from *rho3/rho4* mutants differed little from that in the wild type (10). On the other hand, synthase from the *rho1* mutant showed a decrease in activity, which was not remedied by the addition of GTP- γ -S (Fig. 1A). The defect was evident even when *rho1* cells were grown at the permissive temperature and was exacerbated by incubation of the cells at 37°C. Fraction A (5) restored both activity and GTP- γ -S stimulation to membrane preparations from the *rho1-104* strain (Fig. 1B). The wild-type

Fig. 1. $\beta(1\rightarrow3)$ Glucan synthase defect in *rho1* mutants and reconstitution of the system. In all cases, cells were grown and membrane fractions were prepared and assayed for GS activity as described (5). Results are the average of duplicate determinations that differed less than 10%. The wild-type *RHO1* strain used was OHNY1 (*MAT a ura3 leu2 trp1 his3 ade2*), and the *rho1* mutant strain was HNY21 (*MAT a ura3 leu2 trp1 his3 ade2 rho1-104*). (A) GS activity in wild-type and *rho1-104* membrane



fractions. Cells were grown at 26°C continuously (26°C) or transferred to 37°C for 2 hours (26°→37°C) before harvesting. (B) Reconstitution of GS activity of *rho1-104* with fraction A. The amount of added fraction A was 20 μ g. (C) Reconstitution of GS activity in *rho1-104* with recombinant Rho1p (23). The amount of added Rho1p was 0.7 pmol per reaction mixture. (D) Reconstitution of GS activity with Rho1p and fraction B from strain GS1-36. Fraction B (7.2 μ g of protein) was added to all reaction mixtures.